JOC The Journal of Organic Chemistry

Article

Mechanism of Boron-Catalyzed N-Alkylation of Amines with Carboxylic Acids

Qi Zhang, Ming-Chen Fu, Hai-Zhu Yu, and Yao Fu

J. Org. Chem., **Just Accepted Manuscript** • DOI: 10.1021/acs.joc.6b00778 • Publication Date (Web): 21 Jul 2016

ACS Publications

The Journal of Organic Chemistry is published by the American Chemical Society.
1155 Sixteenth Street N.W., Washington, DC 20036

Mechanism of Boron-Catalyzed N-Alkylation of Amines with Carboxylic Acids

Qi Zhang,[a] Ming-Chen Fu,[a] Hai-Zhu Yu,[*b] Yao Fu [*a]

[a] *Collaborative Innovation Center of Chemistry for Energy Materials, CAS Key Laboratory of Urban Pollutant Conversion, Department of Chemistry, University of Science and Technology of China, Hefei 230026*

[b] *Department of Chemistry and Centre for Atomic Engineering of Advanced Materials, Anhui University, Hefei, 230601*

Emails: fuyao@ustc.edu.cn; yuhaizhu@ahu.edu.cn

Abstract

Mechanistic study has been carried out on the $B(C_6F_5)_3$-catalyzed amine alkylation with carboxylic acid. The reaction includes acid-amine condensation and amide reduction steps. In condensation step, the catalyst-free mechanism is found to be more favorable than the $B(C_6F_5)_3$-catalyzed mechanism, because the automatic formation of the stable $B(C_6F_5)_3$-amine complex deactivates the catalyst in the latter case. Meanwhile, the catalyst-free condensation is constituted by nucleophilic attack and the indirect H_2O-elimination (with acid acting as proton shuttle) steps. After that, the amide reduction undergoes Lewis acid ($B(C_6F_5)_3$-catalyzed mechanism rather than Brønsted acid ($B(C_6F_5)_3$-coordinated HCOOH)-catalyzed one. The $B(C_6F_5)_3$)-catalyzed reduction includes twice silyl-hydride transfer steps, while the first silyl transfer is the rate-determining step of the overall alkylation catalytic cycle. The above condensation-reduction mechanism is supported by control experiments (on both temperature and substrates). Meanwhile, the predicted chemoselectivity is consistent with the predominant formation of the alkylation product (over disilyl acetal product).

1. Introduction

N-alkylated amines are ubiquitous structures in organic synthesis, pharmaceuticals and biological systems.[1] Given the significance of these structures, developing straightforward and economic synthetic methods has become an important research topic.[2] Compared with the traditional substitution reactions of amines with hazardous alkyl halides,[3] transition metal-catalyzed amine alkylation has recently attracted extensive interest.[4] In recent years, Rh,[5] Ir,[6] Ru,[7] Pd[8] etc. catalyzed hydrogenative reduction of imines and enamines has become powerful strategy to prepare N-alkylated amines (Scheme 1A). However, the substrates (imine and enamine) always require additional preparation from carbonyl compounds. With H_2, CO or silane as reductants, Rh,[9] Ir,[10] Ru,[11] Re,[12] Fe,[13] etc. catalyzed reductive amination of carbonyl compounds[14] (aldehydes, ketones, formic acid and CO_2) provides a more straightforward method (Scheme 1B). For example, Beller group[15] successfully achieved the Pt-catalyzed alkylation of the more stable and available carboxylic acid substrates (Scheme 1C). In this context, our group recently reported a metal-free amine alkylation reaction using $B(C_6F_5)_3$ as catalyst and silane as reductant (Scheme 1D).[16] The alkylation of various aromatic and aliphatic amines with formic acid and general carboxylic acid was achieved. In addition, three important commercialized drug molecules, Butenafine, Cinacalcet and Piribedil were easily synthesized through this method.[16]

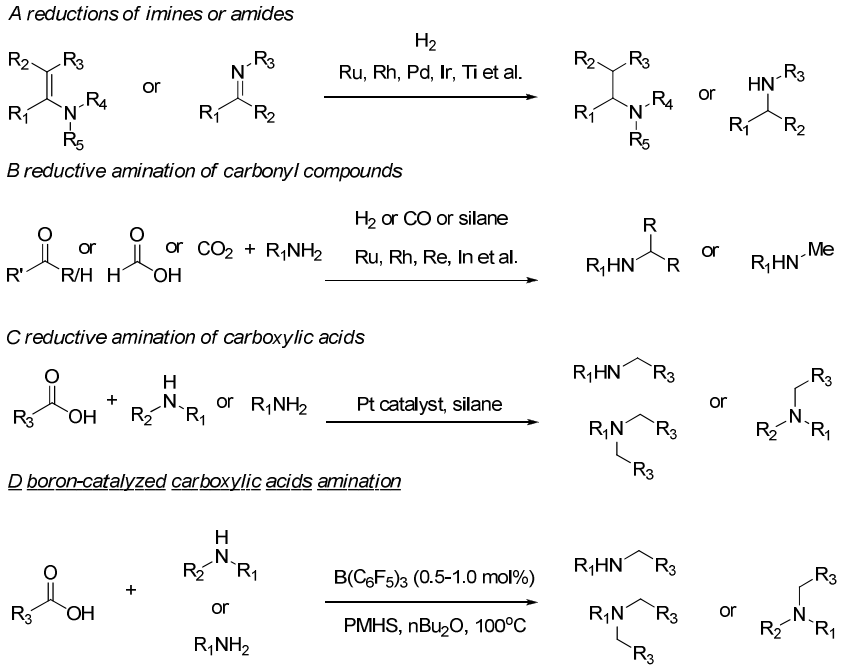

Scheme 1. The synthetic methods of N-alkylated amines

In studying the mechanism of the $B(C_6F_5)_3$-catalyzed amine alkylation, the control experiments indicate that amide is the possible intermediate, rather than aldehyde or alcohol.[16] Accordingly, we proposed that carboxylic acid **1** and amine **2** first undergo condensation to generate amide **3**. Reduction of **3** then occurs to give the alkylation product **4** (Scheme 2A). Nonetheless, there are still some unsolved mechanistic problems. First, the detailed mechanism of the condensation is unclear. According to Whiting's recent study on the condensation reaction between benzoic acid and phenylethylamine,[17] the mechanism mainly undergoes the acid dimerization, nucleophilic attack (with one carboxylic acid acting as proton acceptor) and H_2O-elimination steps (catalyst-free mechanism, Scheme 2B). On the other hand,

Yamamoto[18a] and Brookhart[18b] et al. suggest that $B(C_6F_5)_3$ catalyzed condensation between carboxylic acid and amine might start with a rapid silane-carboxylic acid interaction, and the formed silyl ester then react with amine to generate the amide ($B(C_6F_5)_3$-catalyzed system, Scheme 2B).[19] Both of these two mechanisms are plausible for the condensation step in our reaction system. Second, the mechanism of amide reduction is uncertain. According to the recent studies,[20-24] either Lewis acid or the Brønsted acid ($B(C_6F_5)_3$-coordinated acid) might catalyze the reduction of the carbonyl group (Scheme 2C). Third, the acid was found to be easily reduced to disilyl

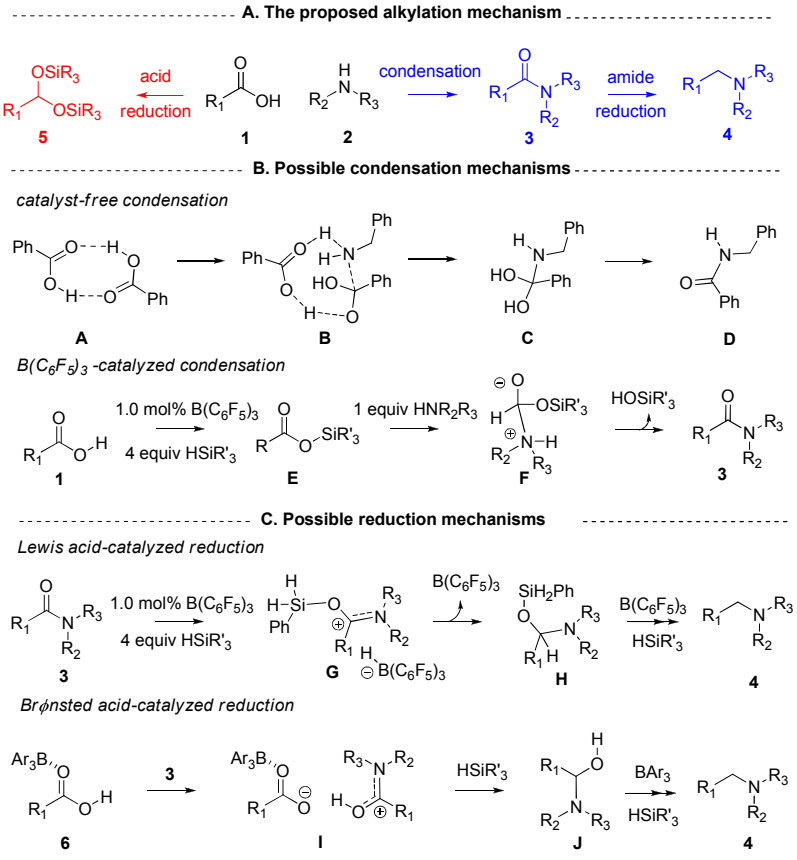

Scheme 2. (A) The possible mechanisms of the boron-catalyzed amine alkylation and acid reduction; (B) The possible condensation mechanisms; (C) The possible reduction mechanisms.

acetal **5** under the $B(C_6F_5)_3$-catalyzed system (Scheme 2A),[18] whereas no disilyl acetal product was observed in our system. The origin for the interesting chemoselectivity is worth clarification. To solve these problems, we carried out combined theoretical and experimental mechanistic studies on the reaction shown in Scheme 1D.

2. Computational methods

The Gaussian09 suite of program[25] was used for calculations in this study. The B3LYP[26-28] method combined with the 6-31G* basis set and SMD model[29] was used for geometry optimization in dibutylether solvent (consistent with our experiments[16]). To get the thermodynamic corrections of Gibbs free energy and verify the stationary points to be local minima or saddle points, we conducted frequency analysis at the same level with optimization. For all transition states, we performed the intrinsic reaction coordinate (IRC) analysis to confirm that they connect the correct reactants and products on the potential energy surfaces.[30] M06-2X[31]/6-311++G** method with the SMD[29] model was used for the solution phase single-point energy calculations of all these stationary points (with dibutylether solvent). All energetics involved in this study are calculated by adding the Gibbs free energy correction calculated at B3LYP/6-31G* and the single-point energy calculated at the M06-2X/6-311++G** method.[32]

3. Results and Discussions

3.1 Model reaction

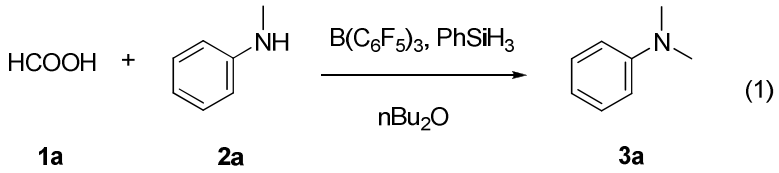

In accordance with our experimental work,[16] the generation of dimethylaniline **3a** by the reaction of formic acid **1a** with methylaniline **2a** (eq 1) is chosen as the model reaction. $B(C_6F_5)_3$, $PhSiH_3$ and nBu_2O are used as catalyst, reductant and solvent, respectively.

3.2 The mechanism of the amine alkylation

Efforts were first put into examining the energy demands of the mechanism of the amine alkylation. In this mechanism, **1a** and **2a** first undergo condensation to generate amide (section 3.2.1), from which reduction occurs to yield the alkylation product **3a** (Section 3.2.2).

3.2.1 The acid-amine condensation

The detailed catalyst-free mechanism. As mentioned in introduction, catalyst-free mechanism includes nucleophilic attack and H_2O-elimination steps.[17] The nucleophilic attack step (Figure 1) starts with the dimerization of carboxylic acid **1a**. The calculation results indicate that the formation of the dimer **Int1** is slightly exergonic by 0.1 kcal/mol, and the two monomers ligate with each other via the hydrogen bonds (Figure 1). After that, the amine substrate **2a** nucleophilically attacks **Int1** via the transition state **TS1** to generate the intermediate **Int2**. In **TS1**, C-N bond formation, and the two proton transfer processes (H transfers from O2 to O, H1

transfers from N to O3, Figure 2) occur simultaneously, and the free energy barrier is 18.2 kcal/mol (**Int1→TS1**).

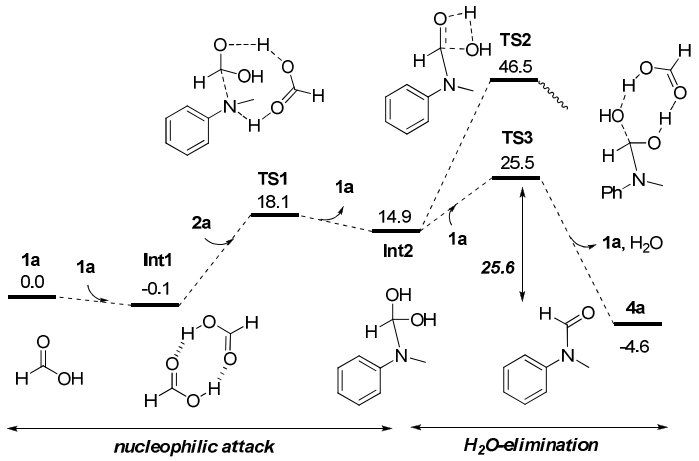

Figure 1. The energy profiles of catalyst-free condensation mechanism (in kcal/mol).

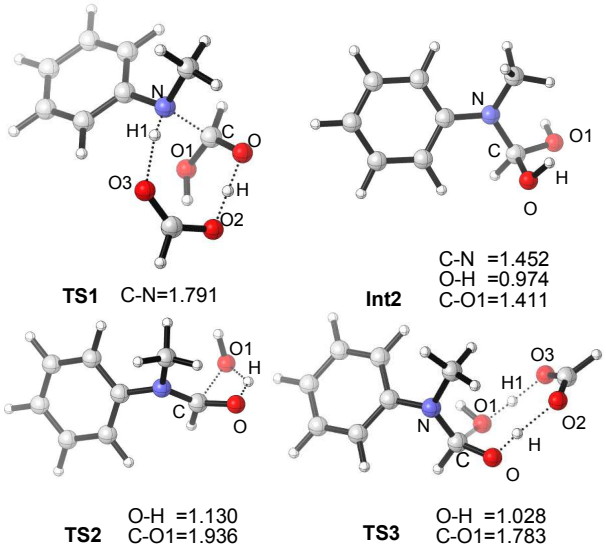

Figure 2. Optimized structures for selected species of Catalyst-free mechanism. Bond lengths are given in Å.

For the H_2O-elimination from **Int2**, we first investigated the direct elimination

mechanism via the transition state **TS2**. In this transition state, the eliminating H, OH group and the forming carbonyl constitute a four-membered ring. The breaking O-H and C-OH bonds stretch to 1.130 and 1.936 Å in **TS2** from 0.974 and 1.411 Å in **Int2** (Figure 2), respectively. The energy barrier for this step is as high as 46.6 kcal/mol (**Int1→TS2**), and thus the possibility for the direct H_2O-elimination can be excluded. Considering that formic acid could possibly act as the proton shuttle,[33] we also examined the energy demand of the indirect H_2O-elimination process. As shown in Figure 1, the two proton transfer processes (H transfers from O to O2, H1 transfers from O3 to O1, Figure 2) and C-O1 cleavage might occur simultaneously via the transition state **TS3**. The breaking O-H bond and C-O1 bond stretch to 1.028 and 1.783 Å respectively. The free energy barrier of the indirect elimination process is 25.6 kcal/mol (**Int1 → TS3**), which is much lower than that of the direct elimination (46.6 kcal/mol). The reason may be attributed to the higher acidity of HCOOH than OH group in **Int2**. After the indirect H_2O-elimination, the amide **4a** was generated. According to the aforementioned discussions, the dimerization-nucleophilic attack-indirect H_2O-elimination represents the feasible catalyst-free condensation mechanism, and the energy demand is 25.6 kcal/mol.

The detailed $B(C_6F_5)_3$-catalyzed mechanism. As mentioned in the introduction, the condensation might also occur via the silyl ester formation, nucleophilic attack and $HOSiR'_3$-elimination steps ($B(C_6F_5)_3$-catalyzed mechanism). According to the calculation results, the coordination of either substrate **1a** or **2a** to the catalyst

$B(C_6F_5)_3$ can stabilize the boron center (Figure 3A), and the coordination is exergonic by 0.9 or 12.3 kcal/mol, respectively. In addition, the generation of proton-transferred intermediate **12a-B** is exergonic by 11.5 kcal/mol. Therefore, **2a-B** is the main existing form of the catalyst, and was chosen as the starting point of the catalyst $B(C_6F_5)_3$.

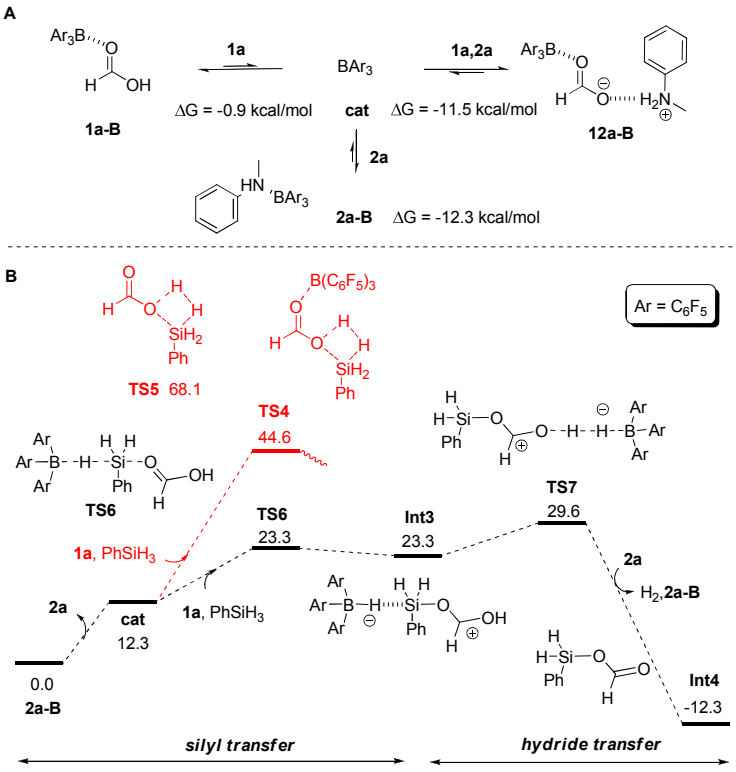

Figure 3. (A) The equilibrium between **cat**, **1a-B**, **2a-B** and **12a-B**; (B) The energy profiles of the silyl ester formation process (in kcal/mol).

Figure 3B shows the detailed energy profiles of the silyl ester formation process. The dissociation of **2a** from **2a-B** occurs first to generate the free catalyst **cat**. $PhSiH_3$ and acid substrate **1a** then participate the silyl transfer step, and the metathesis-type

silyl ester formation was first investigated. In the related transtion state **TS4**, the catalyst $B(C_6F_5)_3$ is coordinated on the carbonyl group of acid, and the breaking O-H of hydroxy and Si-H of $PhSiH_3$ constitute a four-membered ring. The free energy of **TS4** is 44.6 kcal/mol. For comparison, we also located the similar four-membered cyclic transition state **TS5** without the coordination of $B(C_6F_5)_3$. The free energy of **TS5** (68.1 kcal/mol) is significantly higher than **TS4**, indicating that the Lewis acidity of $B(C_6F_5)_3$ benefits the cleavage of O-H bond. Nonetheless, both activation barriers are too high to overcome under the experimental conditions (100^{o}C), and we have to consider the other possibilities.

Inspired by Sakata's recent DFT study[34a] on $B(C_6F_5)_3$-catalyzed ketone hydrosilylation, we took into account the possibility of the $B(C_6F_5)_3$ promoted Si-H cleavage. The energy barrier of the step is 23.3 kcal/mol (**2a-B→TS6**). In the optimized strucutre of **TS6** (Figure 4), the Si-H bond stretches from 1.49 Å (in free $PhSiH_3$) to 1.58 Å, the Si-O and B-H bonds shorten to 2.83 and 1.51 Å, respectively. Therefore, we concluded that the breaking of Si-H bond, formation of Si-O and B-H bonds occur simultaneously. In the generated intermediate **Int3**, the Si-O and B-H bonds further shorten to 2.19 and 1.34 Å, and the Si-H distance stretches to 1.69 Å. From **Int3**, hydride transfer[34] from $HB(C_6F_5)_3^-$ group to the hydroxyl group occurs via the synergistic transition state **TS7**, and the formation of H-H bond, cleavage of O-H and B-H bonds occur simultaneously. This step gives silyl ester intermediate **Int4** and H_2 as the products, and the energy barrier is 29.6 kcal/mol (**2a-B→TS7**). The regenerated catalyst $B(C_6F_5)_3$ then easily coordinates another **2a** to generate the more

stable **2a-B**.

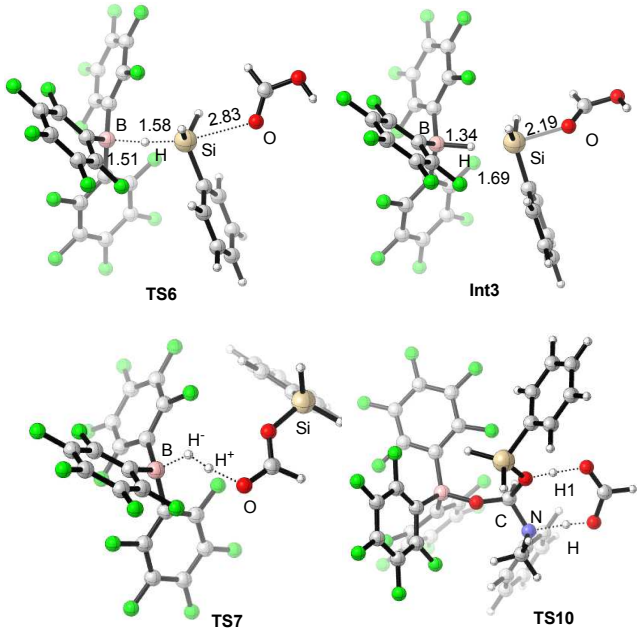

Figure 4. Optimized structures for selected species of $B(C_6F_5)_3$-catalyzed condensation. Bond lengths are given in Å.

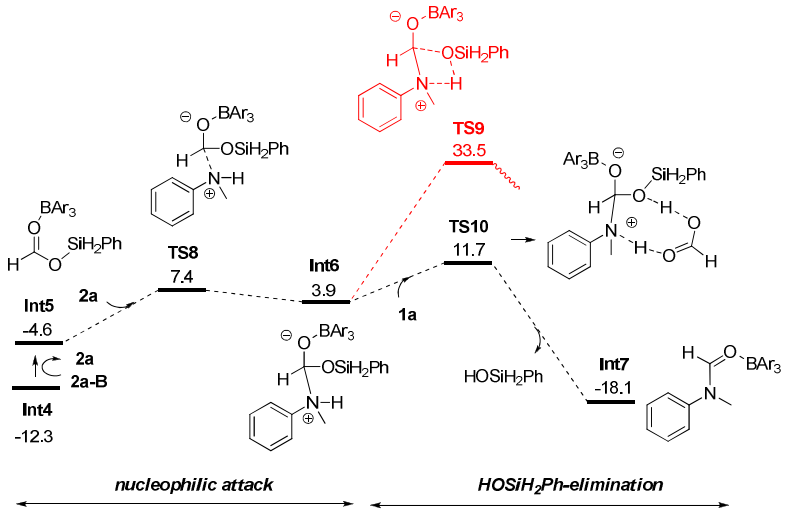

Figure 5. The energy profile of the transformation from silyl ester to amide (in kcal/mol).

From **Int 4**, the energy profiles for the subseqeunt nucleophilic attack and $HOSiH_2Ph$-elimination processes are given in Figure 5. It's found that the $B(C_6F_5)_3$ exchange between **Int4** and **2a-B** in generating $B(C_6F_5)_3$-coordinated silyl ester **Int5** is endergonic by 7.7 kcal/mol. After that, nucleophilic attack of **2a** to **Int5** occurs via the transition state **TS8** with energy barrier of 19.7 kcal/mol (**Int4→TS8**). This step generates the C-N bond formed intermediate **Int6**. For the following $HOSiH_2Ph$-elimination, both the direct elimination and the indirect elimination (with the formic acid as proton shuttle[33]) were investigated. For the direct $HOSiH_2Ph$-elimination process, the free energy of the related four-membered cyclic transition state (i.e. **TS9** in Figures 5) is 33.5 kcal/mol. By contrast, with formic acid acting as proton shuttle, the free energy of the indirect elimination transition state **TS10** is much lower (i.e. 11.7 kcal/mol, Figures 4 & 5). After **TS10**, $HOSiH_2Ph$ is released and the amide **Int7** is formed. The energy barrier of this step is 24.0 kcal/mol (**Int4→TS10**) and the system energy decreases to -18.1 kcal/mol. According to Figures 3 and 5, the energy demand for the $B(C_6F_5)_3$-catalyzed mechanism is 29.6 kcal/mol (**2a-B→TS7**).

Comparison between the catalyst-free and $B(C_6F_5)_3$-catalyzed condensation pathways. Figure 6 shows the comparison between the two possible condensation pathways. For the catalyst-free condensation, nucleophilic attack and H_2O-elimination occur successively to obtain amide **4a** (Figure 1). The indirect H_2O-elimination transition state **TS3** is the highest energy-lying species with free energy of 25.5

kcal/mol (Figure 6). For the $B(C_6F_5)_3$-catalyzed condensation, silyl transfer-hydride transfer process first occurs from **2a-B** to give silyl ester **Int4** (Figure 3), from which nucleophilic attack and $HOSiH_2Ph$-elimination occur to obtain **Int7** (Figure 5). During these processes, the hydride transfer transition state **TS7** is the highest energy-lying species, and its free energy is 29.6 kcal/mol. Therefore, catalyst-free condensation is more favorable than the $B(C_6F_5)_3$-catalyzed one.

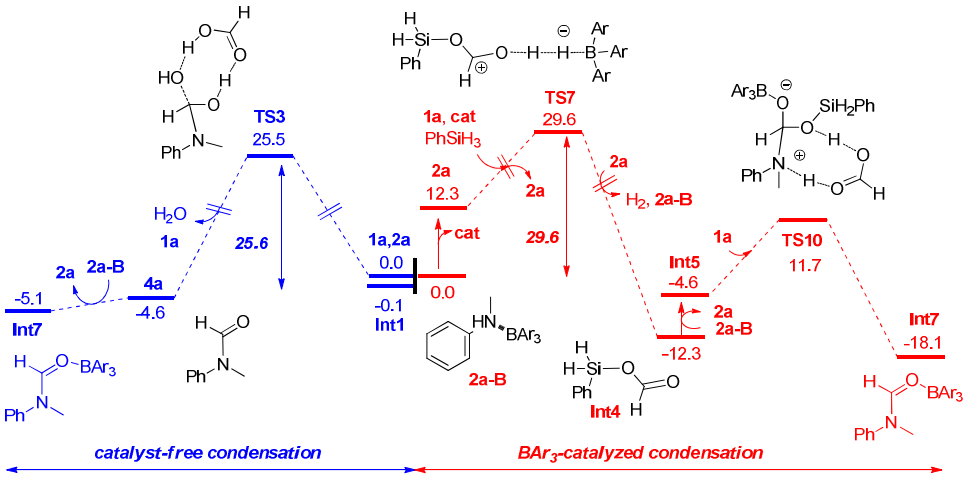

Figure 6. The comparison between the catalyst-free and the $B(C_6F_5)_3$-catalyzed condensation mechanism.

Analyzing the reason for facility of catalyst-free condensation than the $B(C_6F_5)_3$-catalyzed one, we found that the formation of the stable complex **2a-B** is mainly responsible. Without **2a-B**, the energy barrier of $B(C_6F_5)_3$ catalyzed mechanism is only 17.3 kcal/mol (**2a→TS7**). However, the formation of **2a-B** is automatic, as long as the boron catalyst is exposed to the amine substrate **2a**.

Therefore, the coordination passivates the catalyst, and results in the more feasible catalyst-free condensation mechanism.

3.2.2 The reduction of amide

Lewis acid-catalyzed reduction

The detailed energy profiles for the Lewis acid-catalyzed reduction has been shown in Figure 7. $B(C_6F_5)_3$ exchange first occurs between **4a** and **2a-B** to give $B(C_6F_5)_3$-coordinated amide **Int7** and **2a**. From **Int7**, the first silyl transfer occurs via the transition state **TS11** to transfer -$SiPhH_2$ group from silane to carbonyl group of the amide. The energy barrier is 28.4 kcal/mol (**Int7→TS11**). The generated intermediate **Int8** then undergoes hydride transfer transition state **TS12** to transfer H^- from $^-HB(C_6F_5)_3$ group to carbonyl C atom, and the energy barrier is 20.5 kcal/mol (**Int7 → TS12**). After that, the siloxane intermediate **Int9** is generated, and the released catalyst is capped by the amine substrate **2a**. **Int9** then undergoes -$SiPhH_2$ transfer from silane to the O atom of siloxane via the second silyl transfer transition state **TS13**. The generated intermediate **Int10** then easily dissociates **SiOSi** ($PhH_2SiOSiPhH_2$) to generate the imine cation **Int11** and the anion intermediate **Int12**. Finally, a facile hydride transfer occurs between these two intermediates to generate alkylation product **3a** with the regeneration of **2a-B**. According to Figure 7, the first silyl transfer transition state **TS11** determines the overall energy demand of the amide reduction process (28.4 kcal/mol, **Int7→ TS11**).

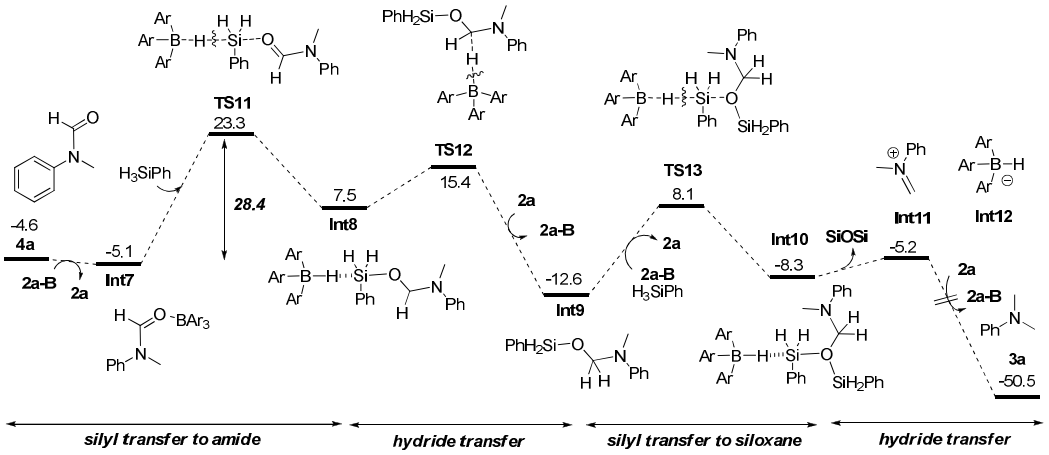

Figure 7. The energy profile of Lewis acid catalyzed amide reduction (in kcal/mol).

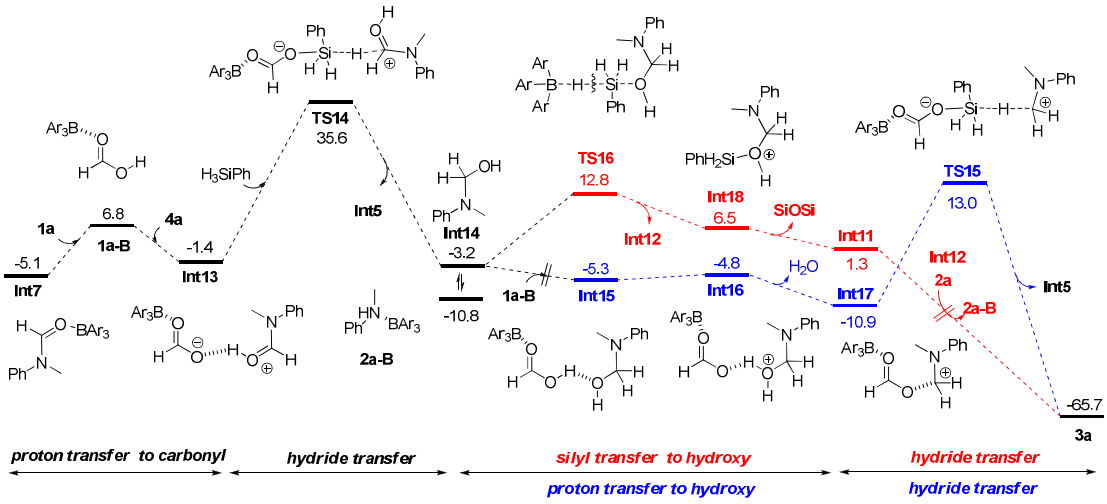

Figure 8. The energy profile of Brønsted acid catalyzed amide reduction (in kcal/mol).

Brønsted acid-catalyzed reduction

Figure 8 shows the detailed energy profiles for the Brønsted acid-catalyzed amide reduction. $B(C_6F_5)_3$ first transfers from **Int7** to **1a**, giving $B(C_6F_5)_3$-coordinated acid **1a-B** as the product. The process is endergonic by 11.9 kcal/mol, because amide is

more nucleophilic than acid. Then, the proton in **1a-B** transfers to the O atom in **4a** to generate **Int13**. The process is barrierless with energy decrease of 8.2 kcal/mol. Subsquently, with the participation of silane, hydride transfer occurs via the transition states **TS14**. In **TS14**, the COO^- group nucleophilicly attacks the Si atom of silane and the hydride of silane transfers to the carbon cation. The energy barrier of the elementary hydride transfer step is 37.0 kcal/mol (**Int13→TS14**). After this step, $B(C_6F_5)_3$-coordinated silyl ester **Int5** and **Int14** are generated with energy decrease of 38.8 kcal/mol. Thereafter, two mechanisms might be responsible for the reduction of **Int14** to the product **3a** (Figure 8). In the Brønsted acid catalyzed reduction (in blue), the proton transfer in intermediate **Int15** first occurs to generate **Int16**. With the release of H_2O, **Int17** is generated with energy decrease of 6.1 kcal/mol. The silane mediated hydride transfer then occurs via the transition state **TS15**. The energy barrier of this step is 23.9 kcal/mol. The product **3a** is finally yielded with **Int5**. In the Lewis acid (i.e. $B(C_6F_5)_3$) catalyzed reduction (in red), **Int14** first goes through silyl transfer transition state **TS16** to generate the intermediate **Int18**. The **Int18** dissociates **SiOSi** to give cation **Int11**. The facile hydride transfer occurs between **Int11** and **Int12** to obtain **3a** and regenerate **2a-B**. The energy barrier of this mechanism is 23.7 kcal/mol (**Int17→TS16**). Therefore, for the reduction of **Int14**, both of these mechanisms are possible (23.9 vs 23.7 kcal/mol). For the overall Brønsted acid-catalyzed amide reduction, the first hydride transfer transition state **TS14** determines the overall energy barrier (40.7 kcal/mol, **Int7→TS14**). It is unfavorable compared with the Lewis acid-catalyzed one (28.4 kcal/mol, Figure 7).

3.3 The overall mechanism of amine alkylation

For clarity reasons, the overall mechanism of the $B(C_6F_5)_3$-catalyzed amine alkylation is shown in Figure 9. The acid **1a** and amine **2a** first undergo the catalyst-free condensation (including nucleophilic attack and H_2O-elimination) to generate amide **4a**. The H_2O-elimination step determines the energy demand of the condensation (25.6 kcal/mol). The following amide reduction undergoes twice silyl transfer-hydride transfer processes to generate alkylation product **3a**. The first silyl transfer determines the energy demand of the amide reduction (28.4 kcal/mol). According to these results, the first silyl transfer in amide reduction is the rate determining step of the amine alkylation reaction, and the overall activation barrier is 28.4 kcal/mol.

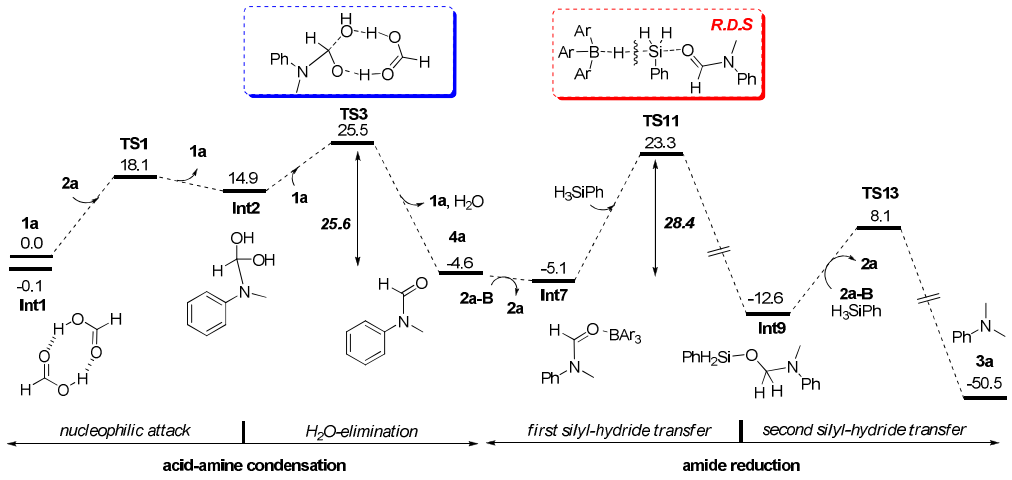

Figure 9. The overall mechanism of the amine alkylation (in kcal/mol).

To verify the above calculation results, some experiments were carried out. First,

condensation product amide were mainly obtained under lowered temperature (eq 2), and this observation is consistent with the calculation results that acid-amine condensation is easier than the amide reduction. Second, without the catalyst $B(C_6F_5)_3$ and reductant $PhSiH_3$, the reaction of **1a** and **2a** gives amide **4a** as the product (eq 3), and this is consistent with the catalyst-free condensation mechanism.[35]

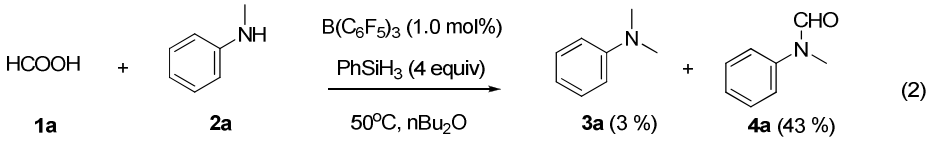

(2)

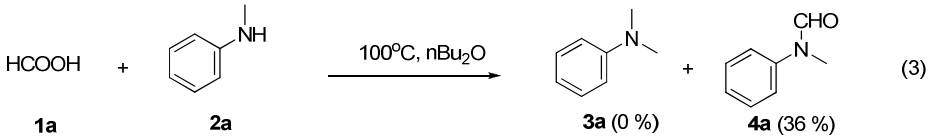

(3)

3.4 Discussions on acid reduction mechanism

According to the previous studies by Yamamoto[18a] and Brookhart [18b], the carboxylic acid could be reduced to disilyl acetal under the $B(C_6F_5)_3$-silane system.[18] Note that our reaction system is highly similar to Yamamoto's, whereas no disilyl acetal was obtained. To explore the origin of the interesting chemoselectivity, we carried out the following calculations and discussions.

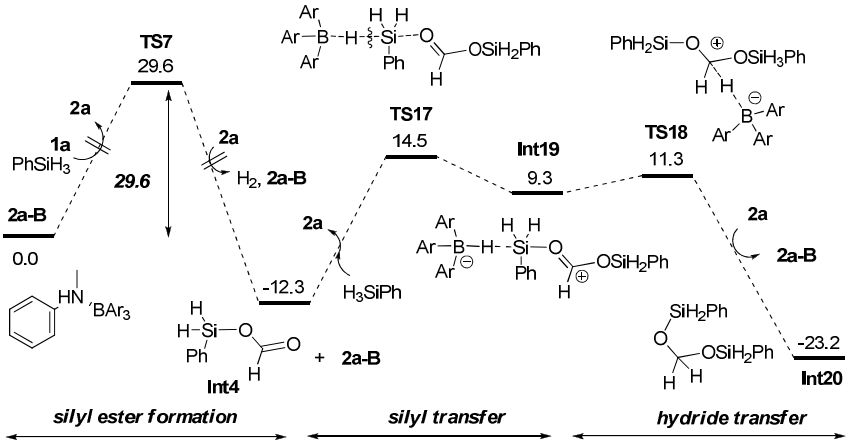

Figure 10. The energy profile of acid reduction process (in kcal/mol).

In our system, the carboxylic acid could be first reduced to the silyl ester (**2a-B + 1a + $PhSiH_3$→Int4**, as shown in Figure 3B), and then the second reduction can occur to obtain the disilyl acetal. The energy barrier for the transformation of **1a** to silyl ester **Int4** is 29.6 kcal/mol. From **Int4**, silyl transfer occurs via transition state **TS17**, transferring the silyl group from silane to the carbonyl in **Int4** to generate intermediate **Int19**. The free energy barrier of this step is 26.8 kcal/mol (**Int4→TS17**). Next, **Int19** undergoes the hydride transfer step to give the disilyl acetal **Int20** via the transition state **TS18**. The free energy barrier of this step is 23.6 kcal/mol (**Int4→TS18**). Accordingly, the transformation from **1a** to **Int20** undergoes twice silyl transfer-hydride transfer processes. The first hydride transfer transition state **TS7** determines the overall energy barrier (29.6 kcal/mol).

Comparing the acid reduction (Figure 10) with amine alkylation (Figure 7), we found that the amide **4a** would be facilely generated, because the acid-amine condensation is stoichiometric and has lower energy barrier than the acid reduction

(25.6 vs 29.6 kcal/mol). From **4a**, the energy barrier of amide reduction is still lower than that of acid reduction (28.4 vs 29.6 kcal/mol). Therefore, the amine alkylation is kinetically more favorable than acid reduction, which is consistent with our previous experiments that alkylation product was obtained predominantly. In addition, the origin of the chemoselectivity is the same as the selectivity origin of the catalyst-free condensation mechanism (over the $B(C_6F_5)_3$-catalyzed one). That is, the formation of the stable amine-$B(C_6F_5)_3$ complex (**2a-B)** passivates the catalyst and results in the unfavorable $B(C_6F_5)_3$-catalyzed acid reduction.

4. Conclusions

Our group recently reported the $B(C_6F_5)_3$-catalyzed carboxylic acid-participated alkylation of various aromatic and aliphatic amines with silane as reductant. In the present study, DFT calculations were carried out to investigate the detailed mechanism. The calculation results show that the condensation of amine and acid undergoes catalyst-free mechanism rather than $B(C_6F_5)_3$-catalyzed mechanism. For the catalyst-free condensation, nucleophilic attack of amine to acid occurs prior to the H_2O-elimination, and indirect elimination process with acid as proton shuttle is the favorable H_2O-elimination mechanism. The following amide reduction undergoes Lewis acid ($B(C_6F_5)_3$)-catalyzed mechanism rather than the Brønsted acid ($B(C_6F_5)_3$-coordinated HCOOH)-catalyzed one. The favorable reduction process includes twice silyl transfer-hydride transfer processes to obtain the alkylation product, with the first silyl transfer acting as the rate-determining step of the overall alkylation

process. The alkylation mechanism is supported by the control experiments of temperature and substrates. Finally, the catalyst passivation caused by the automatic coordination of amine with $B(C_6F_5)_3$ catalyst are determininant to the chemoselectivity, because it results in the unfavorable acid reduction step and the associated $B(C_6F_5)_3$-catalyzed acid reduction mechanisms.

EXPERIMENTAL SECTION

General Procedure. In a Schlenk tube under argon atmosphere, $B(C_6F_5)_3$ (1.0 mol%,1.1 mg) was dissolved in dry $^nBu_2O$ (1.0 mL), and $PhSiH_3$ (4.0 equiv) was added. Then, *N*-Methylaniline (1.0 equiv, 0.2 mmol) and HCO_2H (2.3 equiv, 4.6 mmol) were added via a syringe. The reaction mixture was stirred for 8 h at 100 ^oC. After completion, the mixture was diluted with ethyl acetate (5 mL), quenched with aqueous NaOH (3 M solution; 3 mL) carefully, and stirred for 3 h at room temperature. The yields were analyzed by GC using n-Dodecane as an internal standard.

N,N*-Dimethylaniline (3a):** The compound data was in agreement with the literature (Ref. *Adv. Synth. Catal.* **2015, 357,* 714). ^1H NMR (400 MHz, $CDCl_3$) δ 7.29 – 7.19 (m, 2H), 7.02 – 6.34 (m, 3H), 2.94 (s, 6H).

N*-Methylformanilide (4a)：** The compound data was in agreement with the literature (Ref. *Chem. Commun.,* **2014, 50,* 189). ^1H NMR (400 MHz, $CDCl_3$) δ 8.48 (s, 1H), 7.42 (t, *J* = 7.9 Hz, 1H), 7.35 – 7.26 (m, 1H), 7.22 – 7.15 (m, 1H), 3.33 (s, 1H).

ASSOCIATED CONTENT

Supporting Information

Details of the control experiments, and Cartesian coordinates, free energies, and thermal corrections. The Supporting Information is available free of charge on the ACS Publications website.

AUTHOR INFORMATION

Corresponding Author

fuyao@ustc.edu.cn; yuhaizhu@ahu.edu.cn

Notes

The authors declare no competing financial interests.

ACKNOWLEDGMENT

We thank the NSFC (21325208, 21172209, 21361140372), the 973 Program (2012CB215306), Scientific research funds of Anhui University (J10117700074), FRFCU (WK2060190025, WK2060190040), CAS (KJCX2-EW-J02), PCSIRT and National Supercomputing Center in Shenzhen and USTC for providing the computational resources.

REFERENCES

(1) (a) Nugent, T. C.; El-Shazly, M. *Adv. Synth. Catal.* **2010**, *352*, 753. (b) Wolfe, J. P.; Wagav, S.; Marcoux, J. F.; Buchwald, S. L. *Acc. Chem. Res.* **1998**, *31*, 805.

(2) For reviews, see: (a) Ramirez, T. A.; Zhao, B.; Shi, Y. *Chem. Soc. Rev.* **2012**, *41*,

931. (b) Yadav, J. S.; Antony, A.; Rao, T. S.; Reddy, B. V. S. *J. Organomet. Chem.* **2011**, *696*, 16. (c) Crozet, D.; Urrutigoity, M.; Kalck, P. *ChemCatChem.* **2011**, *3*, 1102. (d) Bähn, S.; Imm, S.; Neubert, L.; Zhang, M.; Neumann, H.; Beller, M. *ChemCatChem.* **2011**, *3*, 1853. (e) Collet, F.; Lescot, C.; Dauban, P. *Chem. Soc. Rev.* **2011**, *40*, 1926. (f) Guillena, G.; Ramon, D. J.; Yus, M. *Chem. Rev.* **2010**, *110*, 1611. (g) Mueller, T. E.; Hultzsch, K. C.; Yus, M.; Foubelo, F.; Tada, M. *Chem. Rev.* **2008**, *108*, 3795. (h) Beauchemin, A. M.; Moran, J.; Lebrun, M.-E.; Seguin, C.; Dimitrijevic, E.; Zhang, L.; Gorelsky, S. I. *Angew. Chem. Int. Ed.* **2008**, *47*, 1410. (i) Salvatore, R. N.; Yoon, C. H.; Jung, K. W. *Tetrahedron* **2001**, *57*, 7785.

(3) (a) Modern Amination Methods (Ed.: A. Ricci), Wiley-VCH, Weinheim, **2007**; (b) Advanced Organic Chemistry, 5th ed. (Ed.: M. B. Smith, J. March), Wiley-Interscience, New York, **2001**.

(4) For reviews, see: (a) Werkmeister, S.; Junge, K.; Beller, M. *Org. Process Res. Dev.* **2014**, *18*, 289. (b) Bezier, D.; Sortais, J.-B.; Darcel, C. *Adv. Synth. Catal.* **2013**, *355*, 19. (c) Xie, J.-H.; Zhu, S.-F.; Zhou, Q.-L. *Chem. Rev.* **2011**, *111*, 1713. (d) Addis, D.; Das, S.; Junge, K.; Beller, M. *Angew. Chem. Int. Ed.* **2011**, *50*, 6004. (e) Nugent, T. C.; El-Shazly, M. *Adv. Synth. Catal.* **2010**, *352*, 753. (f) Das, S.; Zhou, S.; Addis, D.; Enthaler, S.; Junge, K.; Beller, M. *Top. Catal.* **2010**, *53*, 979. (g) Kobayashi, S.; Ishitani, H. *Chem. Rev.* **1999**, *99*, 1069.

(5) (a) Patureau, F. W.; Boer, S. D.; Kuil, M.; Meeuwissen, J.; Breuil, P.-A. R.; Siegler, M. A.; Spek, A. L.; Sandee, A. J.; Bruin, B. D.; Reek, J. N. H. *J. Am. Chem. Soc.* **2009**, *131*, 6683. (b) Gridnev, I. D.; Imamoto, T.; Hoge, G.; Kouchi, M.; Takahashi, H. *J. Am.*

Chem. Soc. **2008**, *130*, 2560. (c) Wang, D.-Y.; Hu, X.-P.; Huang, J.-D.; Deng, J.; Yu, S.-B.; Duan, Z.-C.; Xu, X.-F.; Zheng, Z. *Angew. Chem. Int. Ed.* **2007**, *46*, 7810. (d) Shang, G.; Yang, Q.; Zhang, X. *Angew. Chem. Int. Ed.* **2006**, *45*, 6360. (e) Hou, G.-H.; Xie, J.-H.; Wang, L.-X.; Zhou, Q.-L. *J. Am. Chem. Soc.* **2006**, *128*, 11774. (f) Burk, M. J.; Wang, Y. M.; Lee, J. R. *J. Am. Chem. Soc.* **1996**, *118*, 5142., and references cited therein.

(6) (a) Hou, G.-H.; Xie, J.-H.; Yan, P.-C.; Zhou, Q.-L. *J. Am. Chem. Soc.* **2009**, *131*, 1366. (b) Han, Z.; Wang, Z.; Zhang, X.; Ding, K. *Angew. Chem. Int. Ed.* **2009**, *48*, 5345. (c) Erre, G. E.; Enthaler, S.; Junge, K.; Addis, D.; Beller, M. *Adv. Synth. Catal.* **2009**, *351*, 1437. (d) Zhu, S.-F.; Xie, J.-B.; Zhang, Y.-Z.; Li, S.; Zhou, Q.-L. *J. Am. Chem. Soc.* **2006**, *128*, 12886. (e) Moessner, C.; Bolm, C. *Angew. Chem. Int. Ed.* **2005**, *44*, 7564. (f) Maire, P.; Deblon, S.; Breher, F.; J. Geier, C. Böhler, H. Rüegger, H.Schönberg, H. Grützmacher, *Chem. Eur. J.* **2004**,*10*, 4198. (g) Solinas, M.; Pfaltz, A.; Cozzi, P. G.; Leitner, W. *J. Am. Chem. Soc.* **2004**, *126*, 16142.

(7) (a) Cheruku, P.; Church, T. L.; Andersson, P. G. *Chem. Asian. J.* **2008**, *3*, 1390. (b) Clarke, M. L.; Diaz-Valenzuela, B.; Slawin, A. M.; *Organometallics* **2007**, *26*, 16. (c) Cobley, C. J.; Henschke, J. P. *Adv. Synth. Catal.* **2003**, *345*, 195. (d) Dupau, P.; Bruneau, C.; Dixneuf, P. H. *Adv. Synth. Catal.* **2001**, *343*, 331. (e) Abdur-Rashid, K.; Lough, A. J.; Morris, R. H. *Organometallics* **2001**, *20*, 1047. (f) Noyori, R.; Ohta, M.; Hsiao, Y.; Kitamura, M.; Ohta, T.; Takaya, H. *J. Am. Chem. Soc.* **1986**, *108*, 7117., and references cited therein.

(8) (a) Yu, C.-B.; Wang, D.-W.; Zhou, Y.-G. *J. Org. Chem.* **2009**, *74*, 5633. (b) Wang,

Y.-Q.; Yu, C.-B.; Wang, D.-W.; Wang, X.-B.; Zhou, Y. -G. *Org. Lett.* **2008**, *10*, 2071. (c) Wang, Y.-Q.; Lu, S.-M.; Zhou, Y.-G. *J. Org. Chem.* **2007**, *72*, 3729. (d) Yang, Q.; Shang, G.; Gao, W.; Deng, J.; Zhang, X. *Angew. Chem. Int. Ed.* **2006**, *45*, 3832. (e) Suzuki, A.; Mae, M.; Amii, H.; Uneyama, K. *J. Org. Chem.* **2004**, *69*, 5132. (f) Abe, H.; Amii, H.; Uneyama, K. *Org. Lett.* **2001**, *3*, 313.

(9) (a) Chusov, D.; List, B. *Angew. Chem. Int. Ed.* **2014**, *53*, 5199. (b) Kadyrov, R.; Riermeier, T. H.; Dingerdissen, U.; Tararov, V.; Börner, A. *J. Org. Chem.* **2003**, *68*, 4067. (c) Tararov, V. I.; Kadyrov, R.; Riermeier, T. H.; Börner, A. *Chem. Commun.* **2000**, 1867. (d) Margalef-Català, R.; Claver, C.; Salagre, P.; Fernández, E. *Tetrahedron Lett.* **2000**, *41*, 6583.

(10) (a) Gnanamgari, D.; Moores, A.; Rajaseelan, E.; Crabtree, R. H. *Organometallics* **2007**, *26*, 1226. (b) Mizuta, T.; Sakaguchi, S.; Ishii, Y. *J. Org. Chem.* **2005**, *70*, 2195. (c) Imao, D.; Fujihara, S.; Yamamoto, T.; Ohta, T.; Ito, Y. *Tetrahedron* **2005**, *61*, 6988. (d) Chi, Y.; Zhou, Y.-G.; Zhang, X. *J. Org. Chem.* **2003**, *68*, 4120.

(11) (a) Li, Y.; Fang, X.; Junge, K.; Beller, M. *Angew. Chem. Int. Ed.* **2013**, *52*, 9568. (b) Beydoun, K.; Stein, T. V.; Klankermayer, J.; Leitner, W. *Angew. Chem. Int. Ed.* **2013**, *52*, 9554. (c) Li, Y.; Sorribes, I.; Yan, T.; Junge, K.; Beller, M. *Angew. Chem. Int. Ed.* **2013**, *52*, 12156. (d) Kadyrov, R.; Riermeier, T. H. *Angew. Chem. Int. Ed.* **2003**, *42*, 5472.

(12) (a) Bernardo, J. R.; Sousa, S. C. A.; Florindo, P. R.; Wolff, M.; Machura, B.; Fernandes, A. C. *Tetrahedron* **2013**, *69*, 9145. (b) Das, B. G.; Ghorai, P. *Chem. Commun.* **2012**, *48*, 8276.

(13) (a) Jaafar, H.; Li, H.; Castro, L. C. M.; Zheng, J.; Roisnel, T.; Dorcet, V.; Sortais, J.-B.; Darcel, C. *Eur. J. Inorg. Chem.* **2012**, 3546. (b) Enthaler, S. *ChemCatChem.* **2010**, *2*, 1411.

(14) (a) Sorribes, I.; Junge, K.; Beller, M. *Chem. Eur. J.* **2014**, *20*, 7878. (b) Jacquet, O.; Frogneux, X.; Gomes, C. D. N.; Cantat, T. *Chem. Sci.* **2013**, *4*, 2127. (c) Kumar, V.; Sharma, U.; Verma, P. K.; Kumar, N.; Singh, B. *Adv. Synth. Catal.* **2012**, *354*, 870. (d) Sreedhar, B.; Reddy, P. S.; Devi, D. K. *J. Org. Chem.* **2009**, *74*, 8806. (e) Lee, O.-Y.; Law, K. -L.; Ho, C.-Y.; Yang, D. *J. Org. Chem.* **2008**, *73*, 8829. (f) Robichaud, A.; Ajjau, A. N. *Tetrahedron Lett.* **2006**, *47*, 3633., and references cited therein.

(15) Sorribes, I.; Junge, K.; Beller, M. *J. Am. Chem. Soc.* **2014**, *136*, 14314.

(16) Fu, M. -C.; Shang, R.; Cheng, W.-M.; Fu, Y. *Angew. Chem. Int. Ed.* **2015**, *54*, 9042.

(17) Charville, H.; Jackson, D. A.; Hodges, G.; Whiting, A.; Wilson, M. R. *Eur. J. Org. Chem.* **2011**, 5981.

(18) (a) Gevorgyan, V.; Rubin, M.; Liu, J. X.; Yamamoto, Y. *J. Org. Chem.* **2001**, *66*, 1672. (b) Bézier, D.; Park, S.; Brookhart, M. *Org. Lett.* **2013**, *15*, 496. (c) Feghali, E.; Jacquet, O.; Thuéry, P.; Cantat, T. *Catal. Sci. Technol.* **2014**, *4*, 2230.

(19) The review for Frustrated Lewis Pair: (a) Stephan, D. W.; Erker, G. *Angew. Chem. Int. Ed.* **2015**, *54*, 6400. (b) Stephan, D. W. *Acc. Chem. Res.* **2015**, *48*, 306.

(20) Blondiaux, E.; Cantat, T. *Chem. Commun.* **2014**, *50*, 9349.

(21) Parks, D. J.; Blackwell, J. M.; Piers, W. E. *J. Org. Chem.* **2000,** *65*, 3090.

(22) Rubin, M.; Schwier, T.; Gevorgyan, V. *J. Org. Chem.* **2002**, *67*, 1936.

(23) (a) Doyle, M. P.; DeBruyn, D. J.; Kooistra, D. A. *J. Am. Chem. Soc.* **1972**, *94*, 3659. (b) West, C. T.; Donelly, S.; Kooistra, D. A.; Doyle, M. P. *J. Org. Chem.* **1973**, *38,* 2675. (c) Doyle, M. P.; West, C. T. *J. Org. Chem.* **1975**, *40*, 3835.

(24) (a) Sassaman, M. B.; Kotian, K. D.; Prakash, G. K. S.; Olah, G. A. *J. Org. Chem.* **1987**, *52*, 4314. (b) Sassamann, M. B.; Prakash, G. K. S.; Olah, G. A. *Tetrahedron* **1988**, *44*, 3771.

(25) Frisch, M. J.; Trucks, G. W.; Schlegel, H. B.; Scuseria, G. E.; Robb, M. A.; Cheeseman, J. R.; Scalmani, G.; Barone, V.; Mennucci, B.; Petersson, G. A.; Nakatsuji, H.; Caricato, M.; Li, X.; Hratchian, H. P.; Izmaylov, A. F.; Bloino, J.; Zheng, G.; Sonnenberg, J. L.; Hada, M.; Ehara, M.; Toyota, K.; Fukuda, R.; Hasegawa, J.; Ishida, M.; Nakajima, T.; Honda, Y.; Kitao, O.; Nakai, H.; Vreven, T.; Montgomery, J. A. Jr.; Peralta, J. E.; Ogliaro, F.; Bearpark, M.; Heyd, J. J.; Brothers, E.; Kudin, K. N.; Staroverov, V. N.; Keith, T.; Kobayashi, R.; Normand, J.; Raghavachari, K.; Rendell, A.; Burant, J. C.; Iyengar, S. S.; Tomasi, J.; Cossi, M.; Rega, N.; Millam, J. M.; Klene, M.; Knox, J. E.; Cross, J. B.; Bakken, V.; Adamo, C.; Jaramillo, J.; Gomperts, R.; Stratmann, R. E.; Yazyev, O.; Austin, A. J.; Cammi, R.; Pomelli, C.; Ochterski, J. W.; Martin, R. L.; Morokuma, K.; Zakrzewski, V. G.; Voth, G. A.; Salvador, P.; Dannenberg, J. J.; Dapprich, S.; Daniels, A. D.; Farkas, O.; Foresman, J. B.; Ortiz, J. V.; Cioslowski, J.; Fox, D. J.; Gaussian 09, revision D.01; Gaussian, Inc.: Wallingford CT, 2013.

(26) Becke, A. D. *J. Chem. Phys.* **1993**, *98*, 5648.

(27) Lee, C.; Yang, W.; Parr, R. G. *Phys. Rev. B* **1988**, *37*, 785.

(28) (a) Zhao, H.-T.; Lin, Z.-Y.; Marder, T. B. *J. Am. Chem. Soc.* **2006**, *128*, 15637. (b) Liu, B.; Gao, M.; Dang, L.; Zhao, H.-T.; Marder, T. B.; Lin, Z.-Y. *Organometallics* **2012**, *31*, 3410. (c) Kleeberg, C.; Crawford, A. G.; Batsanov, A. S.; Hodgkinson, P.; Apperley, D. C.; Cheung, M. S.; Lin, Z.-Y.; Marder, T. B. *J. Org. Chem.* **2012**, *77*, 785. (d) Paddon-Row, M. N.; Anderson, C. D.; Houk, K. N. *J. Org. Chem.* **2009**, *74*, 861. (e) Zhang, Q.; Yu, H.-Z.; Shi, J. *Acta Phys.-Chim. Sin.* **2013**, *29*, 2321. (f) Zhang, Q.; Yu, H.-Z.; Fu, Y. *Org. Chem. Front.* **2014**, *1*, 614. (g) Li, Z.; Liu, L.; *Chin. J. Catal.* **2015**, *36*, 3. (h) Shang, R.; Yang, Z.-W.; Wang, Y.; Zhang, S.-L.; Liu, L. *J. Am. Chem. Soc.* **2010**, *132*, 14391.

(29) Hollwarth, A.; Bohme, M.; Dapprich, S.; Ehlers, A. W.; Gobbi, A.; Jonas, V.; Kohler, K. F.; Stegmann, R.; Veldkamp, A.; Frenking, G. *Chem. Phys. Lett.* **1993**, *208*, 237.

(30) Gonzalez, C.; Schlegel, H. B. *J. Phys. Chem.* **1990**, *94*, 5523.

(31) (a) Zhao, Y.; Truhlar, D. G. *Theor. Chem. Acc.* **2008**, *120*, 215. (b) Zhao, Y.; Truhlar, D. G. *Acc. Chem. Res.* **2008**, *41*, 157.

(32) B3LYP// M06-2X method has been frequently used in theoretical studies of organic reaction systems: (a) Um, J. M.; DiRocco, D. A.; Noey, E. L.; Rovis, T.; Houk, K. N. *J. Am. Chem. Soc.* **2011**, *133*, 11249. (b) Krenske, E. H.; Houk, K. N.; Harmata, M. *J. Org. Chem.* **2015**, *80*, 744. (c) Xue, X.-S.; Yang, C.; Li, X.; Cheng, J.-P. *J. Org. Chem.* **2014**, *79*, 1166. (d) McIntosh, G. J.; Russell, D. K. *J. Phys. Chem. A* **2013**, *117*, 4183. (e) Lo, R.; Ganguly, B. *J. Phys. Chem. C* **2013**, *117*, 19325. (f) Flynn, B. L.; Manchala, N.; Krenske, E. H. *J. Am. Chem. Soc.* **2013**, *135*, 9156. (g) McIntosh, G. J.;

Russell, D. K. *J. Phys. Chem. A* **2014**, *118*, 12192.

(33) (a) Qu, S.; Dang, Y.; Song, C.; Guo, J.; Wang, Z.-X. *ACS Catal.* **2015**, *5*, 6386. (b) Clark, J. M.; Nimlos, M. R.; Robichaud, D. J. *J. Phys. Chem. A* **2015**, *119*, 501.

(34) (a) Sakata, K.; Fujimoto, H. *J. Org. Chem.* **2013**, *78*, 12505. (b) Houghton, A. Y.; Hurmalainen, J.; Mansikkamäki, A.; Piers, W. E.; Tuononen, H. M. *Nat. Chem.* **2014**, *6*, 983.

(35) Please see Supporting Information for the experimental details.

Table of Content